He, X., Hsiao, M-S., Boott, C., Harniman, R., Nazemi, A., Li, X., ... Manners, I. (2017). Two-dimensional assemblies from crystallizable homopolymers with charged termini. *Nature Materials*, *16*(4), 481–488. https://doi.org/10.1038/nmat4837

Customized 2D Assemblies from Crystallizable Homopolymers with Charged Termini

Xiaoming He,[1] Ming-Siao Hsiao,[2,#] Charlotte E. Boott,[1,#] Robert L. Harniman,[1,#] Ali Nazemi,[1] Xiaoyu Li,[1,3] Mitchell A. Winnik,[4] and Ian Manners[1,*]

[1]School of Chemistry, University of Bristol, Bristol BS8 1TS, United Kingdom

[2]UES, Inc. and Materials & Manufacturing Directorate, Air Force Research Laboratory, Wright-Patterson AFB, OH 45433, USA

[3]Department of Polymer Materials, School of Material Science and Technology, Beijing Institute of Technology, Beijing 100081, PR China

[4]Department of Chemistry, University of Toronto, Toronto, Ontario M5S 3H6, Canada

[#]These authors contributed equally to this work

[*]To whom correspondence should be addressed: ian.manners@bristol.ac.uk

The creation of shaped, uniform, and colloidally-stable two-dimensional (2D) assemblies by bottom-up methods represents a challenge of widespread current interest for a variety of applications. We describe the utilization of surface charge to stabilize self-assembled planar structures that are formed from crystallizable polymer precursors by a seeded growth approach. Thus, addition of crystallizable homopolymers with charged end groups to seeds generated by the sonication of block copolymer micelles with crystalline cores yields uniform platelet micelles with controlled dimensions. Significantly, the seeded growth approach is characterized by a morphology "memory" effect whereby the origin of the seed, which can involve a quasi-hexagonal or rectangular 2D platelet precursor, dictates the observed 2D platelet shape. The epitaxial nature of the growth process was confirmed in each case by selected area electron diffraction. The new approach was illustrated using two different polymer systems and opens the door to the construction of shaped 2D hierarchical structures with broad utility.

Natural and synthetic two-dimensional (2D) planar structures, as exemplified by clay nanosheets and graphene, respectively, have gained extensive recent attention as a result of their unique properties that originate from their ultrathin and flat morphology.[1-3] "Bottom-up" self-assembly of crystalline homopolymers and block copolymers (BCPs) represents a promising route to analogous 2D materials based on soft matter.[4-7] However, the development of synthetic protocols that permit access to colloidally stable 2D materials with uniform structures and with shape and dimensional control represents a key contemporary challenge.

Crystalline homopolymers generally form 2D thin lamellae which, unless functionalized with solvophilic substituents, are generally not colloidally stable.[8,9] Recent advances have demonstrated the use of thiol-terminated crystalline homopolymers that allow the peripheral nanoparticle patterning on the 2D platelet,[10,11] as well as the fabrication of alternate rings of a homopolymer and BCP.[12,13] In a further advance, nanosheets formed by the crystallization of precursors containing silsesquioxane clusters bound to hyperbranched polymers can be fragmented into seeds using sonication which can be used to control the growth of 2D platelets on subsequent precursor addition.[14]

We have shown that addition of a BCP with a crystallizable poly(ferrocenyldimethylsilane) (PFS) core-forming block[15] and a short complementary corona-forming block to seeds derived from the sonication of 1D cylindrical PFS BCP micelles allows access to lenticular platelet micelles.[16] Sequential addition of different PFS BCPs to seeds yields lenticular platelet block comicelles with concentric regions of different coronal chemistry. In contrast, analogous seeded growth of a crystallizable blend of PFS homopolymer and a PFS BCP with a long corona-forming segment affords rectangular platelet micelles.[17] Moreover, sequential addition of different blends to generate block comicelles followed by spatially selective processing allows their programmed disassembly to yield perforated or hollow rectangular morphologies. In this case, the presence of a corona-forming block of significant length improves the colloidal stability of the resulting 2D structures, but the blend approach adds a degree of complexity because of the need to determine the optimum homopolymer and BCP ratio.

Inspired by the well-established use of electrostatic forces to stabilize particulate dispersions in colloid science, we have explored the use of charged groups in place of coronal chains in the formation of 2D platelets from BCPs using seeded growth processes. We anticipated that incorporation of a charged group at the terminus of a crystalline homopolymer, aggregation of the resulting platelets would be prevented by repulsive forces leading to colloidal stability.

Seeded growth of PFS homopolymers with charged end-groups using 1D seeds

Seeded-growth of crystallizable BCPs from 1D cylindrical seeds prepared by sonication of long, polydisperse cylinders with a crystalline core provides a recently established route to low dispersity cylindrical micelles of controlled length[18-20] and also complex architectures such as block comicelles,[21-23] branched cylindrical micelles,[24] and multi-armed micelles.[25] The key to this approach is that the core termini of the seeds remain active to the addition of further BCP unimer, leading to a process that is analogous to a living covalent polymerization of molecular monomers.[18] Successful implementation relies on the use of core-forming blocks with close crystal lattice matching.[26] Significantly, the resulting micelles are kinetically-trapped as a consequence of the crystallization of the core and the constituent BCP chains are resistant to dynamic exchange between micelles under the conditions used which would otherwise lead to substantial dispersities in length.

In order to explore the use of a charged terminal group in place of a corona-forming block we have studied the seeded growth of a near monodisperse PFS homopolymer possessing a degree of polymerization of 20 and with terminal phosphonium groups and iodide counteranions, $PFS_{20}[PPh_2Me]I$ (Fig. 1). This material was prepared by methylation of a neutral precursor, $PFS_{20}PPh_2$. Addition of a solution of molecularly dissolved (unimeric) $PFS_{20}[PPh_2Me]I$ in THF to long cylindrical PFS_{25}-*b*-$P2VP_{250}$ micelle seeds (P2VP = poly(2-vinylpyridine), the subscripts refer to the number average degree of polymerization) of number average length L_n = 840 nm (length dispersity L_w/L_n = 1.03, L_w is the weight average length) in *i*PrOH afforded highly uniform rectangular platelet micelles (Fig. 2a and Supplementary Fig. 1). The area of the platelets was found to be linearly dependent on the unimer-to-seed mass ratio (m_{unimer}/m_{seed}) and the area dispersity was very low (A_w/A_n = 1.02, where A_w is the weight-average area and A_n is the number-average area). Significantly, the platelet micelles were readily dispersible in *i*PrOH and the solution was colloidally stable, with no evidence for a change in size or shape or for precipitation after three months. The aspect ratio (L_n/W_n) was found to decrease non-linearly (from 14.0 to 4.1) upon increasing the ratio of m_{unimer}/m_{seed} (from 4 to 40) (Supplementary Fig. 1j), indicating the preferential tendency for growth in the lateral direction (perpendicular to the seed axis).

As shown in Fig. 2a, transmission electron microscopy (TEM) clearly indicated that the PFS_{25}-*b*-$P2VP_{250}$ seed was located at the center of the platelets as a dark region of high electron density as a consequence of seeded-growth both at the seed ends and the seed sides. Unlike our previous report on the formation of lenticular micelles using seeded growth of BCPs, preferential growth off the ends of

the cylinder was not observed.[16] The facile lateral growth observed may be a consequence of the lower steric demands of $PFS_{20}[PPh_2Me]I$. Thus, the absence of long coronal chains may minimize the hindrance to lateral addition expected from the corona of the cylindrical PFS_{25}-*b*-$P2VP_{250}$ seed micelles. The heights of the platelet and the central cylindrical seed by atomic force microscopy (AFM) were found to be 10 nm and 20 nm, respectively (Supplementary Fig. 1c). The larger height of the central seed is at least partly attributed to presence of corona chains. Given that the average distance between two adjacent main chain iron centers in a PFS chain is 0.65 nm,[27] the extended chain length of PFS_{20} is calculated to be 13 nm. Therefore in the 2D platelet structure surrounding the seed, the PFS chains appear to be extended with a single fold and interdigitated, perpendicular to the planar surface.

To characterize the positive surface of the platelets, a zeta potential measurement (Supplementary Fig. 3) was performed for a sample of rectangular 2D assemblies in *i*PrOH (L_n = 1955 nm, W_n = 348 nm). This gave a positive value of +35 mV, indicative of the presence of a positive surface which would be expected to provide good colloidal stability.[28] These platelet micelles with a positively charged surface function as a template for loading and patterning negatively charged nanostructures, such as silica nanoparticles (Supplementary Fig. 4, see supplementary information for further discussion). In order to clarify the importance of a terminal positive charge on the formation of uniform and colloidal stable platelet micelles from the seeded growth of $PFS_{20}[PPh_2Me]I$, a control experiment was carried out using neutral analogue $PFS_{20}PPh_2$. Following the same protocol of addition of a unimer solution of $PFS_{20}PPh_2$ in THF to the cylindrical PFS_{25}-*b*-$P2VP_{250}$ seeds (L_n = 840 nm, L_w/L_n = 1.03) in *i*PrOH, very different results were obtained. Unlike the colloidally stable 2D platelets formed from the seeded growth of $PFS_{20}[PPh_2Me]I$, obvious precipitation was observed on addition of $PFS_{20}PPh_2$ in THF to the same PFS_{25}-*b*-$P2VP_{250}$ seeds in *i*PrOH. Moreover, TEM indicated that irregular 2D plate structures formed with uncontrolled aggregation (Supplementary Fig. 5). This indicated that the introduction of a charged group at the terminus of the homopolymer is necessary to permit the colloidal stability required for a controlled growth process.

The addition of $PFS_{20}[PPh_2Me]I$ in THF to shorter PFS_{25}-*b*-$P2VP_{330}$ seeds (L_n = 58 nm, L_w / L_n = 1.02) in *i*PrOH also led to the formation of 2D rectangular platelets with the aspect ratio showing a similar trend of decreasing values (from 7.6 to 4.3) as the m_{unimer}/m_{seed} ratio increased (from 4 to 20) (Supplementary Fig. 6). However, the aspect ratio for the platelets formed by the shorter seeds was significantly smaller. This indicated that the dimensions of the 2D rectangular platelets can be

controlled by seed length and the m_{unimer}/m_{seed} ratio. Moreover, providing that the solvent is suitably adjusted, the system is tolerant to considerable mismatches in the degrees of polymerization of the PFS segments in the unimer and seed and also the counteranion used (Supplementary Fig. 7 and 8, see supplementary information for further details). The generality of the method was also illustrated by the observation that BCPs with a charged terminus, such as PFS BCP PI_{25}-*b*-$PFS_{22}[PPh_2Me]I$, with a short isoprene (PI) block at one end and a charged phosphonium group at the other, also formed well-defined rectangular platelets via seeded growth in *i*PrOH (Supplementary Fig. 9). Furthermore, the use of a PFS homopolymer with a negatively charged terminus, PFS_{20}-SO_3Li, also led to the formation of rectangular platelets using 1D cylindrical seeds further illustrating the pervasive nature of this new approach (Supplementary Fig. 10).

Seeded growth of PFS homopolymers with charged end-groups using 2D seeds

In the absence of cylindrical seeds, addition of $PFS_{20}[PPh_2Me]I$ in THF to *i*PrOH resulted in the formation of a precipitate of aggregated large 2D platelets (Supplementary Fig. 11a). The platelets formed were more colloidally stable in MeOH and were found to possess a disk-like morphology (Supplementary Fig. 11b). Sonication led to cleavage into small, polydisperse platelet fragments (A_n = 7985 nm^2, A_w/A_n = 1.53; Supplementary Fig. 12). Next, we explored the seeded growth of $PFS_{20}[PPh_2Me]I$ using these 2D seeds (2D $Seed_{HD}$; where the subscript 'HD' refers to the quasi-hexagonal disk-like morphology of the seed precursor) as initiators. Interestingly, addition of unimer $PFS_{20}[PPh_2Me]I$ in THF to the 2D $seed_{HD}$ in MeOH led to the formation of monodisperse, quasi-hexagonal disk-like 2D structures (Fig. 2b and Supplementary Fig.13), reminiscent of the platelet aggregate precursors (Supplementary Fig. 11b). Similar quasi-hexagonal disk-like 2D platelets can also be prepared via seeded growth in *i*PrOH (Supplementary Fig. 14). As for the case of the rectangular platelet analogues, the area of these quasi-hexagonal disk-like platelets also followed a linear relationship to the m_{unimer}/m_{seed} ratio (Supplementary Fig. 13). With increasing unimer, the disk-like platelets become increasingly uniform, with the polydispersity decreasing from 1.54 for the small 2D seeds before unimer addition to 1.03 (m_{unimer}/m_{seed} = 40). AFM analysis indicated that these disks are very flat, the average height of *ca.* 10 nm, again suggesting a interdigitated structure with a single chain fold (Supplementary Fig. 13f-g).

The quasi-hexagonal disk-like platelets synthesized by the seeded growth method share a similar morphology with their "parent" 2D aggregates used to form the seeds. Such a "memory" effect is a likely consequence of identical crystal packing in these 2D structures and also the preference for

similar growth rates in the different crystallographic directions (see further discussions below and in the Supplementary Information page S10).[29] We envisaged that if the 2D seeds possess a "memory" of the shape of the "parent" platelets, it should be possible to prepare 2D platelets using 2D seeds derived from platelets of different shape. We therefore explored the use of 2D seeds derived from the rectangular platelets (Fig. 2a) prepared using cylindrical seed precursors. By sonication of the "parent" rectangular platelets, the 1st generation of 2D seeds was obtained (2D $Seed_{R1}$, Supplementary Fig. 15; where the subscript R1 refers to the rectangular morphology and seed generation). Subsequent addition of a unimer solution $PFS_{20}[PPh_2Me]I$ in THF to the 2D $Seed_{R1}$ in MeOH afforded uniform rectangular platelets of well-controlled size (Fig. 2c and Supplementary Fig. 16). Very few quasi-hexagonal platelets (< 5 %) were present in the sample. Furthermore, we also found that the "memory" was maintained in the 2nd generation of the 2D rectangular seeds (2D $Seed_{R2}$, Supplementary Fig. 15) which was prepared by sonication of the rectangular platelets formed by the addition of unimeric $PFS_{20}[PPh_2Me]I$ in THF to 2D $Seed_{R1}$ in MeOH. Once again, rectangular platelets of controlled dimensions could be prepared by varying the ratio of $PFS_{20}[PPh_2Me]I$ unimer to the 2D $Seed_{R2}$ (Supplementary Fig. 17). AFM analysis showed that the rectangular platelets grown from 2D $Seed_{R1}$ and 2D $Seed_{R2}$ were very flat with a height of 10 nm (Supplementary Fig. 16b-c). In contrast to the rectangular platelets with cylindrical seeds at the center, the aspect ratio of the rectangular platelet grown from 2D rectangular seeds possessed an almost constant value of *ca.* 2 irrespective of the m_{unimer}/m_{seed} ratio. Analogous rectangular platelets with a similar aspect ratio can also be prepared from 2D rectangular seeds via seeded growth in *i*PrOH (Supplementary Fig. 18).

Significantly, the seeded growth method we describe here is compatible with previously reported seeded growth approaches that use BCPs and homopolymer/BCP blends and allows the preparation of complex hierarchical structures.[16,17] Moreover, the use of 2D platelets of different shape as building blocks permits an additional level of control. For example, addition of the polymer blend (PFS_{25}/PFS_{25}-*b*-$P2VP_{250}$ = 1:1 based on mass ratio) to quasi-hexagonal disk-like platelets (grown from 2D $seed_{HD}$) or 2D rectangular analogues (prepared either from 1D PFS_{25}-*b*-$P2VP_{250}$ seeds or 2D $seed_{R1}$) yielded block coplatelets in which the precursor shape was retained (Fig. 3). AFM images showed the obvious height difference where the second block with PFS_{25}/PFS_{25}-*b*-$P2VP_{250}$ polymer blend has 20 nm higher than the first block. By sequential alternating addition of a PFS_{25}/PFS_{25}-*b*-$P2VP_{250}$ blend (1:1, mass ratio) and $PFS_{20}[PPh_2Me]I$, concentric segmented platelet comicelles with four distinct regions of excellent contrast were formed based on TEM (Supplementary Fig. 19).

Although morphology "memory" is well-established for the growth of 2D semiconducting nanosheets through epitaxial growth,[30,31] reports involving soft matter are much less common.[13,29] Furthermore, to our knowledge, the use of different seeds from the same polymer to induce the formation of 2D platelets of different shape via seeded growth in solution is unprecedented. Analysis by selected area electron diffraction (SAED) analysis revealed that the quasi-hexagonal disk-like and rectangular platelets (grown from 2D $seed_{HD}$ and 2D $seed_{R1}$, respectively) have near identical ED patterns with three pairs of diffraction spots, confirming the presence of a single crystalline PFS core with monoclinic symmetry (Fig. 4 and Supplementary Fig 20).[27,32] The formation of isotropic disk-like quasi-hexagonal or anisotropic rectangular shaped platelet micelles is attributed to the difference in growth rate[33] along the (110), (100) and (010) normal of the crystalline PFS core (Fig 4, see supplementary information page S10 for additional discussion).[34,35] The growth rate of the planes (G(hkl)) for disk-like quasi-hexagonal platelets follows the trend G(010) >>> G(100) = G(110) while for rectangular plates, the growth rate follows the order G(110) >>> G(100) = G(010). Electron diffraction analysis for the spatially distinct regions of 2D platelet block comicelles with different shapes confirmed that the crystalline structure for the PFS core was identical in each case (Fig. 4, Supplementary Fig. 20), confirming the epitaxial nature of the growth process.

In order to confirm that self-assembly occurred in the solution phase rather than on solvent evaporation and to monitor the formation of the different segments, laser scanning confocal microscopy (LSCM) was used to characterize platelets formed in solution from PFS homopolymers end-functionalized with a green fluorescent dye, PFS_{22}-G (Fig. 1). Via addition of a blend of $PFS_{20}[PPh_2Me]I$ and PFS_{22}-G (10:1, mass ratio) to quasi-hexagonal disk-like or rectangular platelets, very uniform fluorescent almost circular, quasi-hexagonal or rectangular rings were prepared (Supplementary Fig. 22).

The use of platelet micelles with different shapes as initiators enables the formation of hierarchical and complex structures. Addition of the BCP PFS_{20}-*b*-$P2VP_{140}$ with a long corona-forming block to the rectangular platelet (prepared from 1D PFS_{25}-*b*-$P2VP_{250}$ seed) in *i*PrOH led to scarf-like structures, where the added BCP grew as the tassel fibers selectively at both long-axis termini (Supplementary Fig. 23a). Amphiphilic 2D scarf-like structure can be similarly accessed by addition of PFS_{25}-*b*-$PMVS_{170}$ unimer with a hydrophobic corona-forming segment in *i*PrOH/hexane (3:1, v/v) (Supplementary Fig. S23c). Interestingly, increasing the polarity of the solvent induced the 2D amphiphilic objects to form oligomers via a type of step-growth polymerization process through

favorable hydrophobic interactions of the tassels. Similar scarf-like structures can also be prepared upon addition of PFS_{20}-*b*-$P2VP_{140}$ unimer to rectangular platelets grown from 2D $seed_{R1}$ (Supplementary Fig. 24a). When quasi-hexagonal disk-like platelets were used as initiators, however, addition of PFS_{20}-*b*-$P2VP_{140}$ led to unusual, kinked micelles with less direction selectivity (Supplementary Fig. 24b). Moreover, cross-shape platelets can be fabricated by seeded growth of $PFS_{20}[PPh_2Me]I$ from cylindrical cross-shape micelles prepared from the self-assembly of amphiphilic cylindrical triblock comicelles M(PFS-*b*-PtBA)-*b*-M(PFS-*b*-PDMS)-*b*-M(PFS-*b*-PtBA) (Supplementary Fig. 25).[36]

Concept Extension to Polylactide Homopolymers

In order to explore the generality of the new seeded growth approach to shaped 2D assemblies that utilises homopolymers with charged terminal groups, we applied an analogous design strategy to a semicrystalline organic polymer,[37] poly(*L*-lactide) (PLLA).[19,38,39] Two homopolymers with phosphonium groups at a chain terminus were prepared, $PLLA_{24}[PPh_2Me]I$ and $PLLA_{34}[PPh_2Me]I$ (see Fig. 1). To create suitable seeds, unimer solutions of $PLLA_{24}[PPh_2Me]I$ and $PLLA_{34}[PPh_2Me]I$ were added to polar solvents (such as *i*PrOH or MeOH). In a mixture of *i*PrOH (or MeOH) and $CHCl_3$ (10:1, v/v), formation of aggregates of 2D diamond-shape platelets of variable size (final c = 0.1 mg/mL) was observed at 23 °C in 2 h based on TEM analysis (Supplementary Fig. 26).

The controlled fabrication of uniform 2D PLLA platelets was also achieved by seeded growth. Sonication of 2D platelet of $PLLA_{24}[PPh_2Me]I$ (0.1 mg/mL) in *i*PrOH/$CHCl_3$ (10:1) produced relatively small, almost 1D fragments of low dispersity that function as seeds (L_n = 200 nm, L_w/L_n = 1.09; Supplementary Fig. 27) whereas under the same conditions sonication of the 2D platelet of $PLLA_{34}[PPh_2Me]I$ in *i*PrOH/$CHCl_3$ (10:1) gave 2D seeds with large size and high polydispersity (A_n = 13,980 nm^2, A_w/A_n = 1.75). By using MeOH in place of *i*PrOH, relatively small, lower dispersity 2D seeds of $PLLA_{34}[PPh_2Me]I$ (A_n = 6542 nm^2, A_w/A_n = 1.38; Supplementary Fig. 28) were successfully obtained. Addition of unimeric $PLLA_{24}[PPh_2Me]I$ in $CHCl_3$ to the almost 1D seeds of $PLLA_{24}[PPh_2Me]I$ in *i*PrOH gave very uniform 2D diamond platelets with controlled size obtained by varying the m_{unimer}/m_{seed} (Fig. 5). The vast majority (over 95 %) of the formed platelets were found to have clearly visible 1D seed present at the center by TEM. This indicated that 2D platelet formation involving seeded-growth with the virtual absence of spontaneous nucleation as a competing process. The 2D diamond platelet structure was also confirmed by AFM (Fig. 5f). The average height of the platelets was about 10 nm, and the central seed and four edges were found to be ca. 3 nm higher than

the remaining regions (12 nm vs 9 nm). Analogous to the seeded-growth for the $PFS_{20}[PPh_2Me]I$, the area of the platelets was found to linearly dependent on the m_{unimer}/m_{seed} (Fig. 5h, Supplementary Table 4). Seeded growth of $PLLA_{34}[PPh_2Me]I$ from 2D seeds of $PLLA_{34}[PPh_2Me]I$ also resulted in 2D diamond-shaped platelets (Supplementary Fig. 29). In addition, polymer $PLLA_{34}[PPh_2Me]I$ with a different polymer chain length could also be successfully grown into diamond platelets from 1D seeds of $PLLA_{24}[PPh_2Me]I$, indicating the adaptability of the seeded growth process. By addition of a blend of $PLLA_{24}[PPh_2Me]I$ and $PLLA_{21}$-G (or $PLLA_{21}$-R) (10:1, mass ratio) to a solution of diamond-shaped platelets of $PLLA_{24}[PPh_2Me]I$ (where $PLLA_{21}$-G and $PLLA_{21}$-R refer to PLLA homopolymer end-functionalized with green and red fluorescent dyes, respectively, Fig. 1), concentric fluorescent 2D diamond platelet multiple block comicelles with spatially defined regions of fluorescence were prepared, further illustrating the versatility of the process (Fig. 5j-k).

Conclusions

In summary, we report a simple approach to the preparation of uniform, colloidally stable 2D platelets with different shapes from homopolymers with charged end-groups by a combination of seeded-growth and morphology "memory" effect. A variety of morphologies, such as rectangular, quasi-hexagonal, and diamond platelet micelles have been fabricated for two different polymeric materials. The seeded growth process is likely to be extendable to a wide range of crystallizable polymers, including π-conjugated and biodegradable materials,[19,23] and allows precise control of dimensions and access to hierarchical 2D segmented comicelles and also other complex architectures. The resulting shaped 2D platelets possess a lipophilic charged surface and offer potential applications as carriers for nanoparticles, biomolecules, and therapeutic agents, as liquid crystals and adhesives, and in composite reinforcement. Many of these areas of prospective utility are currently under investigation in our laboratory.

Acknowledgements

X.M.H., A.N. and X.L. are grateful to the European Union (EU) for Marie Curie Postdoctoral Fellowships. C.E.B. thanks the Bristol Chemical Synthesis Centre for Doctoral Training, founded by the Engineering and Physical Sciences Research Council (EPSRC), for a PhD studentship. M.A.W. thanks the Natural Sciences and Engineering Research Council (NSERC) of Canada for financial support. I.M. thanks the EPSRC for support. PeakForce atomic force microscopy was carried out in the Chemical Imaging Facility, University of Bristol with equipment funded by EPSRC. Dr. George

R. Whittell is thanked for helpful discussions.

Author contributions

X.M.H and I.M. conceived the project with input from A.N. X.M.H. synthesized the polymers, performed the experiments. X.M.H. and C.E.B. performed the LSCM imaging. X.M.H. and R.L.H. performed the AFM analysis. X.L. provided the PFS_{25}-*b*-$P2VP_{250}$ seeds. M.S.H. performed the imaging and analysis of ED and EDS mapping. X.M.H., M.S.H. and I.M. prepared the manuscript with input from all the other authors. The project was supervised by I. M.

Additional information

Supplementary information is available in the online version of the paper. Reprints and permissions information is available online at www.nature.com/reprints. Correspondence and requests for materials should be addressed to I. M.

Competing financial interests

The authors declare no competing financial interests.

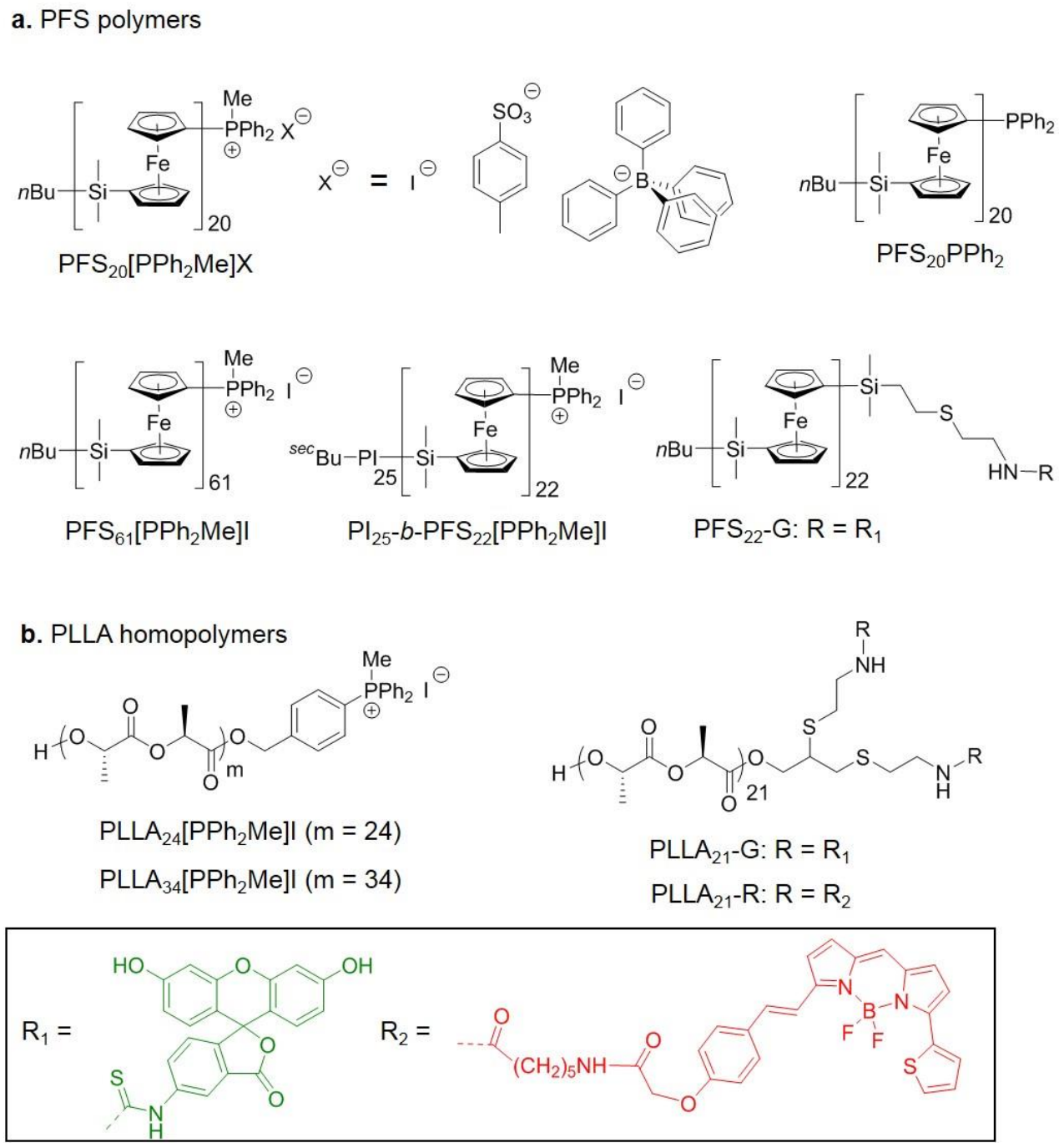

Figure 1 | Chemical structures of homopolymers used for seeded growth.

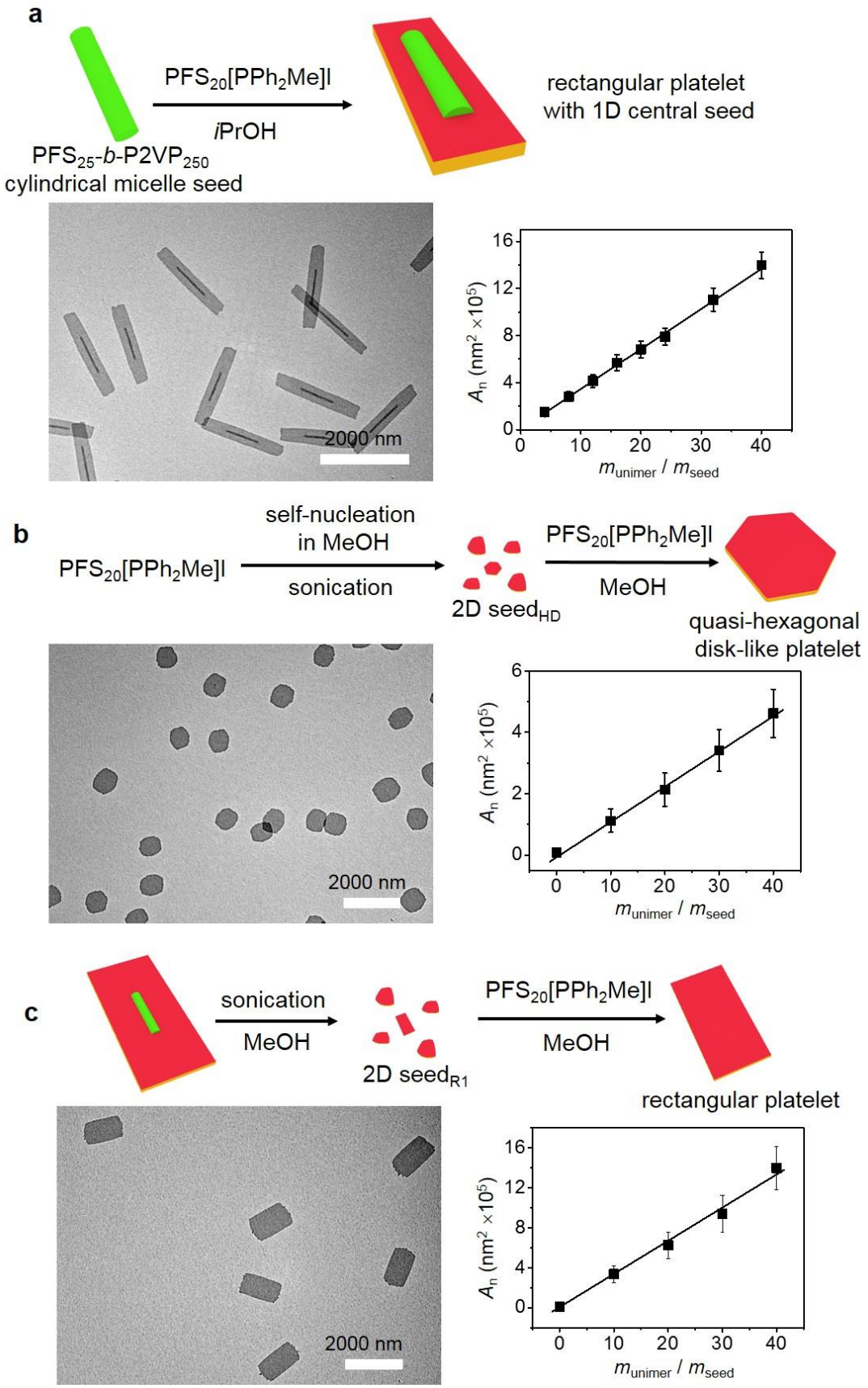
a
PFS20[PPh2Me]I
iPrOH
PFS25-b-P2VP250
cylindrical micelle seed
rectangular platelet
with 1D central seed
2000 nm
An (nm2 ×105)
munimer / mseed
b
PFS20[PPh2Me]I
self-nucleation
in MeOH
sonication
2D seedHD
PFS20[PPh2Me]I
MeOH
quasi-hexagonal
disk-like platelet
2000 nm
An (nm2 ×105)
munimer / mseed
c
sonication
MeOH
2D seedR1
PFS20[PPh2Me]I
MeOH
rectangular platelet
2000 nm
An (nm2 ×105)
munimer / mseed

Figure 2 | Formation of 2D platelet micelles with different morphologies and controlled area prepared by seeded growth of $PFS_{20}[PPh_2Me]I$. a. Schematic representation of the formation of 2D rectangular platelets through seeded growth of $PFS_{20}[PPh_2Me]I$ from 1D cylindrical seeds. TEM images of a representative sample prepared by the seeded growth of unimer $PFS_{20}[PPh_2Me]I$ in THF from PFS_{25}-*b*-$P2VP_{250}$ seed micelles (L_n = 840 nm, L_w / L_n = 1.03) in *i*PrOH at 23 °C, with unimer to seed mass ratios (m_{unimer}/m_{seed}) of 20:1. Linear dependence of micelle area on the m_{unimer}/m_{seed}. Error bars, standard deviation of measured areas. **b**. Schematic representation of the generation of 2D $Seed_{HD}$ and formation of uniform quasi-hexagonal disk-like platelet through seeded growth. TEM images of a representative sample formed through seeded growth of unimer $PFS_{20}[PPh_2Me]I$ in THF from 2D $seed_{HD}$ in MeOH at 23 °C, with m_{unimer}/m_{seed} of 40:1. Linear dependence of micelle area on the m_{unimer}/m_{seed}. Error bars, standard deviation of measured areas. **c**. Schematic representation of the 1st generation of 2D rectangular seed (2D $Seed_{R1}$) and formation of uniform rectangular platelet through seeded growth. TEM images of a representative sample formed through seeded growth of unimer $PFS_{20}[PPh_2Me]I$ in THF from 2D $seed_{R1}$ in MeOH at 23 °C, with m_{unimer}/m_{seed} of 40:1. Linear dependence of micelle area on the m_{unimer}/m_{seed}. Error bars, standard deviation of measured areas.

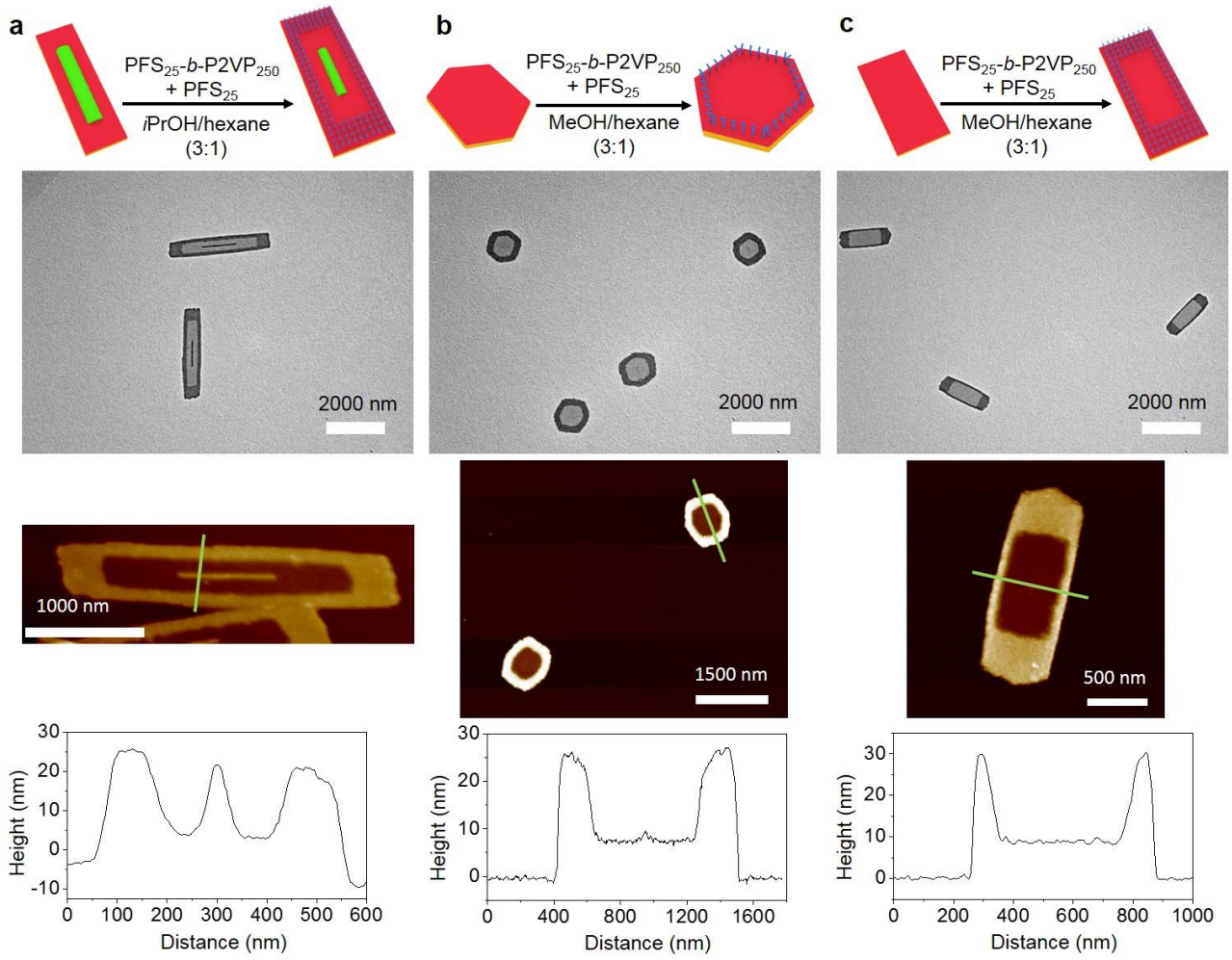

Figure 3 | Formation of platelet block comicelles of different shape. a-c, Schematic representation, TEM images, AFM topography images and corresponding height profiles of block comicelles with 2D morphologies of (a) rectangular platelet grown from 1D PFS_{25}-*b*-$P2VP_{250}$ seed, (b) quasi-hexagonal disk-like platelet grown from 2D $seed_{HD}$ and (c) rectangular platelet grown from 2D $seed_{R1}$. These platelet block comicelles were prepared by addition of PFS_{25}-*b*-$P2VP_{250}$/PFS_{25} (1:1, mass ratio) blend unimer in THF to three types 2D platelets which were formed by the addition of $PFS_{20}[PPh_2Me]I$ unimer in THF to 1D PFS-*b*-$P2VP_{250}$ seed in *i*PrOH/hexane (3:1, v/v), and 2D $seed_{HD}$ or 2D $seed_{R1}$ in MeOH/hexane (3:1, v/v) at 23 °C.

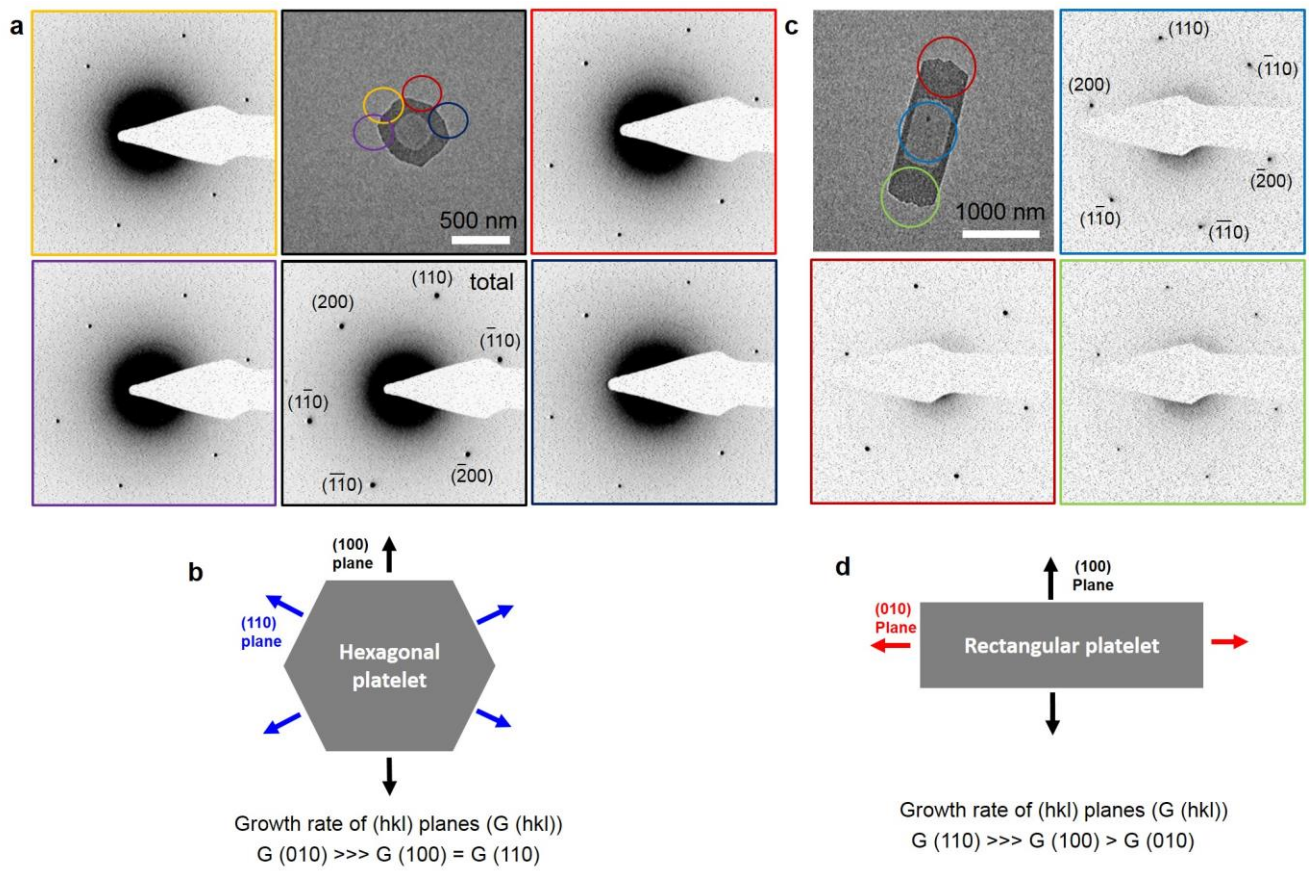

Figure 4 | Selected area electron diffraction (SAED) pattern for platelet block comicelles. a,b. TEM image and SAED patterns for a quasi-hexagonal disk-like platelet block comicelle (a), as well as the schematic representation of the growth mechanism for the micelle and block comicelle including four blue arrows presenting the growth direction of the (110) planes and two black arrows indicating the growth direction of the (100) planes (b). **c,d.** TEM image and SAED patterns for a rectangular platelet block comicelle (c), as well as the schematic representation of the growth mechanism for the micelle and block comicelle containing two red arrows presenting the growth direction of the (010) planes and two black arrows indicating the growth direction of the (100) planes. Exhaustion of the faster growing (110) planes first during crystal growth leads to an absence of (110) facets in a rectangular platelet (d). The platelet block comicelles were prepared by addition of PFS_{25}-*b*-$P2VP_{250}/PFS_{25}$ (1:1, mass ratio) blend unimer in THF to 2D quasi-hexagonal disk-like or rectangular platelets which were formed by the addition of $PFS_{20}[PPh_2Me]I$ unimer in THF to 2D $seed_{HD}$ or 2D $seed_{R1}$ in MeOH/hexane (3:1, v/v) at 23 °C. G indicates the growth direction of the platelet.

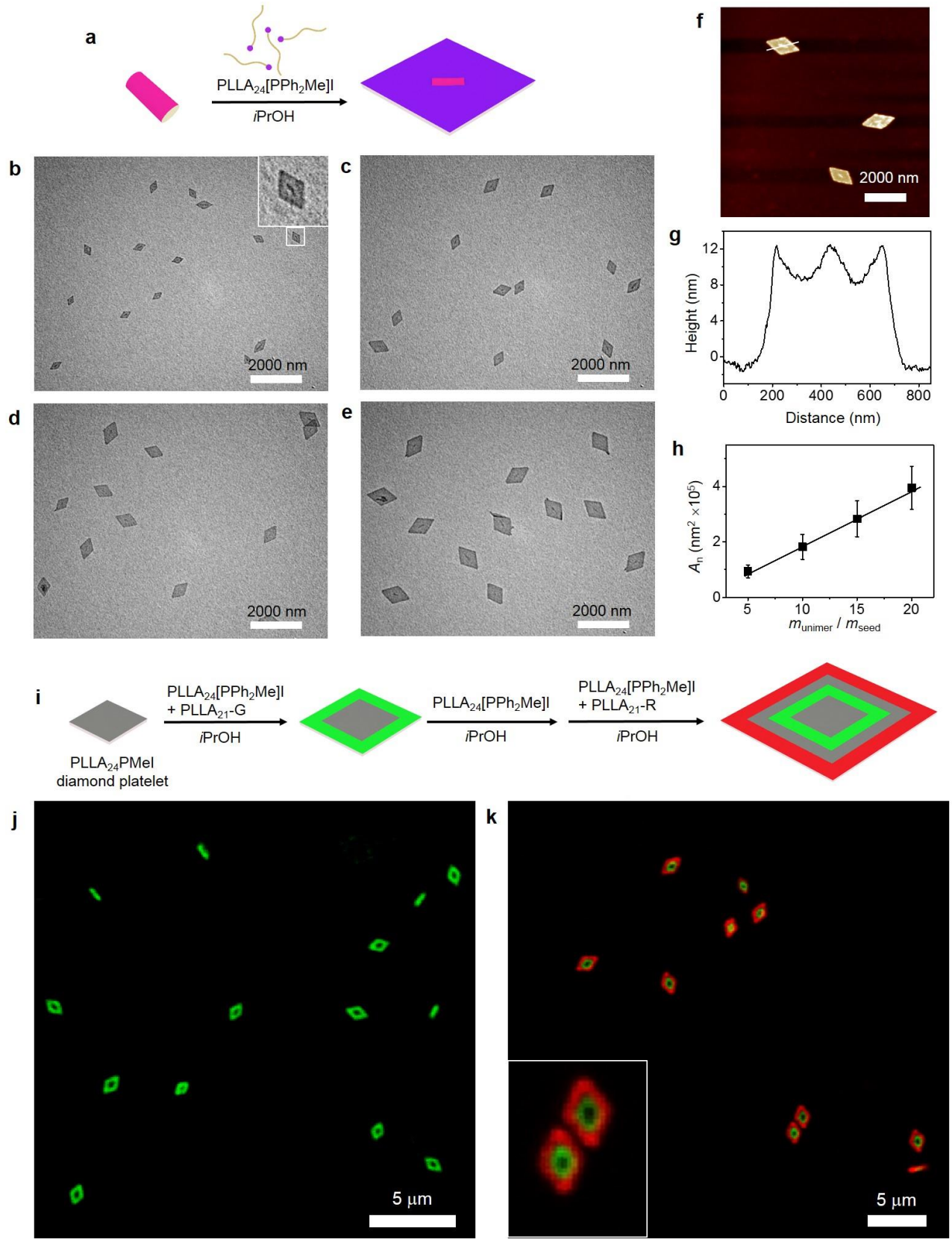

Figure 5 | Uniform diamond platelet micelles of controlled area prepared by seeded growth of PLLA$_{24}$[PPh$_2$Me]I. a, Schematic representation of the formation of diamond platelets through

seeded growth**. b-e**, TEM images of uniform diamond platelets formed through seeded growth from a 1D seed with m_{unimer}/m_{seed} of 5:1 (b), 10:1 (c), 15:1 (d), 20:1 (e). **f**, AFM topography image of a diamond platelet micelle formed from a 20:1 unimer:seed mass ratio. **g**, Height profile of the diamond platelet from AFM. **h**, Linear dependence of micelle area on the m_{unimer}/m_{seed}. Error bars, standard deviation of measured areas. **i.** Schematic diagram showing the formation of fluorescent concentric diamond block co-micelles in 2D from a non-fluorescent diamond platelet (A_n= 182150 nm^2, A_w/A_n = 1.06) by the sequential addition of fluorescent blend ($PLLA_{24}[PPh_2Me]I$ / ($PLLA_{21}$-G or $PLLA_{21}$-R), 10:1 mass ratio) and non-fluorescent $PLLA_{24}[PPh_2Me]I$ in $CHCl_3$ and visualized by LSCM. **j-k**, LSCM images of di-block (j) and tetra-block (k) co-micelles with segregated regions comprised of non-fluorescent block and fluorescent block.

References

1. Zhang, X. & Xie, Y. Recent advances in free-standing two-dimensional crystals with atomic thickness: design, assembly and transfer strategies. *Chem. Soc. Rev.* **42**, 8187-8199 (2013).
2. Boott, C.E., Nazemi, A. & Manners, I. Synthetic Covalent and Non-Covalent 2D Materials. *Angew. Chem. Int. Ed.* **54**, 13876-13894 (2015).
3. Zhuang, X., Mai, Y., Wu, D., Zhang, F. & Feng, X. Two-Dimensional Soft Nanomaterials: A Fascinating World of Materials. *Adv. Mater.* **27**, 403-427 (2015).
4. Rizis, G., van de Ven, T.G.M. & Eisenberg, A. "Raft" Formation by Two-Dimensional Self-Assembly of Block Copolymer Rod Micelles in Aqueous Solution. *Angew. Chem. Int. Ed.* **53**, 9000-9003 (2014).
5. Yang, J.-X*., et al.* Hydrogen-Bonding-Mediated Fragmentation and Reversible Self-assembly of Crystalline Micelles of Block Copolymer. *Macromolecules* **49**, 367-372 (2016).
6. Lee, I.-H*., et al.* Nanostar and Nanonetwork Crystals Fabricated by in Situ Nanoparticlization of Fully Conjugated Polythiophene Diblock Copolymers. *J. Am. Chem. Soc.* **135**, 17695-17698 (2013).
7. Yin, L. & Hillmyer, M.A. Disklike Micelles in Water from Polyethylene-Containing Diblock Copolymers. *Macromolecules* **44**, 3021-3028 (2011).
8. Keller, A. Polymer single crystals. *Polymer* **3**, 393-421 (1962).
9. Geil, P. Polymer Single Crystals. *Robert Krieger Pub. Huntington, NY Press* (1973).
10. Li, B. & Li, C.Y. Immobilizing Au Nanoparticles with Polymer Single Crystals, Patterning and Asymmetric Functionalization. *J. Am. Chem. Soc.* **129**, 12-13 (2007).
11. Dong, B., Zhou, T., Zhang, H. & Li, C.Y. Directed Self-Assembly of Nanoparticles for Nanomotors. *ACS Nano* **7**, 5192-5198 (2013).
12. Chen, W.Y*., et al.* "Chemically Shielded" Poly(ethylene oxide) Single Crystal Growth and Construction of Channel-Wire Arrays with Chemical and Geometric Recognitions on a Submicrometer Scale. *Macromolecules* **37**, 5292-5299 (2004).
13. Zheng, J.X*., et al.* Onsets of Tethered Chain Overcrowding and Highly Stretched Brush Regime via Crystalline−Amorphous Diblock Copolymers. *Macromolecules* **39**, 641-650 (2006).
14. Yu, B., Jiang, X. & Yin, J. Size-Tunable Nanosheets by the Crystallization-Driven 2D Self-Assembly of Hyperbranched Poly(ether amine) (hPEA). *Macromolecules* **47**, 4761-4768 (2014).
15. Hailes, R.L.N., Oliver, A.M., Gwyther, J., Whittell, G.R. & Manners, I. Polyferrocenylsilanes: synthesis, properties and applications. *Chem. Soc. Rev.*, DOI: 10.1039/c1036cs00155f (2016).
16. Hudson, Z.M*., et al.* Tailored hierarchical micelle architectures using living crystallization-driven self-assembly in two dimensions. *Nat. Chem.* **6**, 893-898 (2014).
17. Qiu, H*., et al.* Uniform patchy and hollow rectangular platelet micelles from crystallizable polymer blends. *Science* **352**, 697-701 (2016).
18. Gilroy, J.B*., et al.* Monodisperse cylindrical micelles by crystallization-driven living self-assembly. *Nat. Chem.* **2**, 566-570 (2010).
19. Petzetakis, N., Dove, A.P. & O'Reilly, R.K. Cylindrical micelles from the living crystallization-driven self-assembly of poly(lactide)-containing block copolymers. *Chem. Sci.* **2**, 955-960 (2011).

20. Schmelz, J., Karg, M., Hellweg, T. & Schmalz, H. General Pathway toward Crystalline-Core Micelles with Tunable Morphology and Corona Segregation. *ACS Nano* **5**, 9523-9534 (2011).
21. Wang, X.*, et al.* Cylindrical Block Copolymer Micelles and Co-Micelles of Controlled Length and Architecture. *Science* **317**, 644-647 (2007).
22. Schmelz, J., Schedl, A.E., Steinlein, C., Manners, I. & Schmalz, H. Length Control and Block-Type Architectures in Worm-like Micelles with Polyethylene Cores. *J. Am. Chem. Soc.* **134**, 14217-14225 (2012).
23. Qian, J.*, et al.* Uniform, High Aspect Ratio Fiber-like Micelles and Block Co-micelles with a Crystalline π-Conjugated Polythiophene Core by Self-Seeding. *J. Am. Chem. Soc.* **136**, 4121-4124 (2014).
24. Qiu, H.*, et al.* Branched micelles by living crystallization-driven block copolymer self-assembly under kinetic control. *J. Am. Chem. Soc.* **137**, 2375-2385 (2015).
25. Qiu, H., Cambridge, G., Winnik, M.A. & Manners, I. Multi-Armed Micelles and Block Co-micelles via Crystallization-Driven Self-Assembly with Homopolymer Nanocrystals as Initiators. *J. Am. Chem. Soc.* **135**, 12180-12183 (2013).
26. Gadt, T., Ieong, N.S., Cambridge, G., Winnik, M.A. & Manners, I. Complex and hierarchical micelle architectures from diblock copolymers using living, crystallization-driven polymerizations. *Nat. Mater.* **8**, 144-150 (2009).
27. Gilroy, J.B.*, et al.* Probing the Structure of the Crystalline Core of Field-Aligned, Monodisperse, Cylindrical Polyisoprene-block-Polyferrocenylsilane Micelles in Solution Using Synchrotron Small- and Wide-Angle X-ray Scattering. *J. Am. Chem. Soc.* **133**, 17056-17062 (2011).
28. Hanaor, D., Michelazzi, M., Leonelli, C. & Sorrell, C.C. The effects of carboxylic acids on the aqueous dispersion and electrophoretic deposition of ZrO2. *J. Eur. Ceram. Soc.* **32**, 235-244 (2012).
29. Xu, J., Ma, Y., Hu, W., Rehahn, M. & Reiter, G. Cloning polymer single crystals through self-seeding. *Nat. Mater.* **8**, 348-353 (2009).
30. Tan, C. & Zhang, H. Epitaxial Growth of Hetero-Nanostructures Based on Ultrathin Two-Dimensional Nanosheets. *J. Am. Chem. Soc.* **137**, 12162-12174 (2015).
31. Huang, X.*, et al.* Solution-phase epitaxial growth of noble metal nanostructures on dispersible single-layer molybdenum disulfide nanosheets. *Nat. Commun.* **4**, 1444 (2013).
32. Hsiao, M.-S., Yusoff, S.F.M., Winnik, M.A. & Manners, I. Crystallization-Driven Self-Assembly of Block Copolymers with a Short Crystallizable Core-Forming Segment: Controlling Micelle Morphology through the Influence of Molar Mass and Solvent Selectivity. *Macromolecules* **47**, 2361-2372 (2014).
33. Passaglia, E. & Khoury, F. Crystal growth kinetics and the lateral habits of polyethylene crystals. *Polymer* **25**, 631-644 (1984).
34. Chen, Z.*, et al.* Structure of Poly(ferrocenyldimethylsilane) in Electrospun Nanofibers. *Macromolecules* **34**, 6156-6158 (2001).
35. Papkov, V.S.*, et al.* Crystalline Structure of Some Poly(ferrocenylenedialkylsilylenes). *Macromolecules* **33**, 7107-7115 (2000).
36. Li, X.*, et al.* "Cross" Supermicelles via the Hierarchical Assembly of Amphiphilic Cylindrical Triblock Comicelles. *J. Am. Chem. Soc.* **138**, 4087-4095 (2016).
37. He, W.-N. & Xu, J.-T. Crystallization assisted self-assembly of semicrystalline block copolymers. *Prog. Polym. Sci.* **37**, 1350-1400 (2012).

38. Sun, L.*, et al.* Structural reorganization of cylindrical nanoparticles triggered by polylactide stereocomplexation. *Nat. Commun.* **5**(2014).
39. Sun, L.*, et al.* Core functionalization of semi-crystalline polymeric cylindrical nanoparticles using photo-initiated thiol-ene radical reactions. *Polym. Chem.* **7**, 2337-2341 (2016).